

Fermilab

Energy-momentum tensor in the 2D Ising CFT in full modular space

FERMILAB-CONF-25-0057-T

arXiv:2502.00512

This manuscript has been authored by Fermi Forward Discovery Group, LLC under Contract No. 89243024CSC000002 with the U.S. Department of Energy, Office of Science, Office of High Energy Physics.

Energy-momentum tensor in the 2D Ising CFT in full modular space

Richard C. Brower,^a George T. Flemming,^b Nobuyuki Matsumoto^{a,*} and Rohan Misra^a

^a*Boston University, Boston, MA 02215, USA*

^b*Fermi National Accelerator Laboratory, Batavia, Illinois, 60510, USA*

E-mail: nmatsum@bu.edu

A set of lattice operators for the energy-momentum (EM) tensor in the Ising CFT is derived in the spin variables. Our expression works under arbitrary affine transformation both on triangular and hexagonal lattices (where the former includes the rectangular lattices). The correctness of the operators is numerically confirmed in Monte Carlo calculations by comparing the results with the conformal Ward identity, including the operator normalization. In the derivation of the EM tensor, a staggered structure of the affine-transformed hexagonal lattice is analyzed, which shows a peculiar shift from the circumcenter dual lattice and appears as a mixing angle between the holomorphic part $T(z)$ and the antiholomorphic part $\tilde{T}(\bar{z})$. The details of this contribution will appear in a subsequent paper.

The 41st International Symposium on Lattice Field Theory (LATTICE2024)
28 July - 3 August 2024
Liverpool, UK

*Speaker

1. Introduction

To expand the non-perturbative understanding of quantum field theory, the Quantum Finite Elements (QFE) project [1] aims to enable lattice calculation on curved spacetime. Such an extension enables us to, for example, use radial quantization for conformal field theories (CFTs) in the spacetime with dimensions $D > 2$ [2–4]. As a step towards its rigorous formulation, this work considers the energy-momentum (EM) tensor in the 2D CFT on the torus with generic modulus τ , which is a key physical object that generates diffeomorphism. We derive a lattice expression of the EM tensor in both fermionic and spin variables. The expression is confirmed in direct Monte Carlo calculation by checking the conformal Ward identities [5, 6]. Although we are not the first people who address the EM tensor in the two-dimensional Ising spin model [7], we derive a complete expression including normalization that works under an arbitrary affine transformation. To our knowledge, our work is the first work that verifies the analytic formulas for the Ising CFT involving the EM tensor numerically with the spin variables. The details of the content will be given in a subsequent paper [8].

2. Affine-transformed lattice

We consider a generic affine-transformed triangular lattice as shown in Fig. 1. We write the

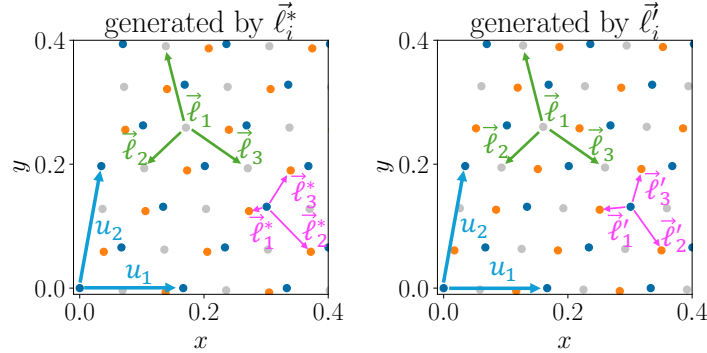


Figure 1: Gray dots represent the affine-transformed triangular lattice. The blue and orange points represent its dual lattices, where the colors distinguish the even (blue) and odd (orange) sites. The left panel shows the circumcenter dual lattice, generated by $\vec{\ell}_i^*$, while the right panel shows the lattice generated by $\vec{\ell}_i$, on which the fields reside (see Sec. 4).

Cartesian coordinates as $(x_\mu) \equiv (x, y)$ and the three lattice translation vectors as $\vec{\ell}_k$ ($k = 1, 2, 3$). The circumcenter dual of the triangular lattice is a hexagonal lattice, and we write the three lattice translation vectors from even to odd sites as $\vec{\ell}_k^*$. We further define the unit vectors on the hexagonal lattice: $\vec{e}_k \equiv \vec{\ell}_k^*/|\vec{\ell}_k^*| \equiv (\cos \alpha_k, \sin \alpha_k)^T$. Depending on the context, we use an alternative notation such as $\vec{\ell}_{nm}^*$ for the lattice translation vector from the site n to m .

We impose periodicity of the torus by the identification:

$$0 \sim L_1 \vec{u}_1 \sim L_2 \vec{u}_2 \quad (L_1, L_2 \in \mathbb{Z}), \quad (1)$$

where $\vec{u}_1 \equiv -2\vec{\ell}_1^* + \vec{\ell}_2^* + \vec{\ell}_3^*$ and $\vec{u}_2 \equiv -\vec{\ell}_1^* - \vec{\ell}_2^* + 2\vec{\ell}_3^*$. In this work, we set $L_1 = L_2 \equiv L$ for simplicity. As we consider a conformal theory on the torus, the scale of the system can be conventionally fixed

by setting one of the lattice dimension to unity: $L|\vec{u}_1| = 1$. With the standard identification between the two-dimensional vector and the complex variable: $\mathbb{R}^2 \simeq \mathbb{C}$, $\vec{u} = (u_x, u_y)^T \leftrightarrow u \equiv u_x + iu_y$, the modulus of the torus can be expressed as $\tau \equiv Lu_2$.

3. Partition functions

As is well known, the 2D Ising model has a fermionic description with the Majorana fermion [9–11]. For later discussion, we consider the Wilson-Majorana fermion action [12, 13] on the hexagonal lattice in a generalized setup with arbitrary couplings:

$$S_W = \frac{1}{2} \sum_n (1 + \Delta m_n) \bar{\psi}_n \psi_n - \sum_{\langle n, m \rangle} \kappa_{nm} \bar{\psi}_n P(\vec{e}_{nm}) \psi_m, \quad (2)$$

where $\psi \equiv (\psi_1, \psi_2)^T$ is the two-component real Grassmann variable, $\langle n, m \rangle$ denotes the nearest neighbor pair, and $P(\vec{e})$ is the Wilson projector:

$$P(\vec{e}) \equiv \frac{1}{2} (1 - \vec{e} \cdot \vec{\sigma}). \quad (3)$$

We use the Pauli matrices $\vec{\sigma} \equiv (\sigma_1, \sigma_2)$ as the gamma matrices throughout the paper. The partition function for the lattice fermion is then:

$$Z_W^{\text{hex}} \equiv \int \mathcal{D}\psi e^{-S_W}, \quad \mathcal{D}\psi \equiv \prod_n d\psi_n^1 d\psi_n^2. \quad (4)$$

Our main focus is the Ising spin system on triangular and hexagonal lattices, whose partition functions are:

$$Z_I^{\text{tri}} \equiv \sum_{\{s_k = \pm 1\}} \exp \left[\sum_{\langle k, \ell \rangle} L_{k\ell} s_k s_\ell \right], \quad (5)$$

$$Z_I^{\text{hex}} \equiv \sum_{\{\mu_n = \pm 1\}} \exp \left[\sum_{\langle n, m \rangle} K_{nm} \mu_n \mu_m \right]. \quad (6)$$

The partition functions (4), (5) and (6) can be related to each other by loop expansions [14, 12, 13] even under various boundary conditions on the torus. For the discussion below, it suffices to quote the following identities:

$$\frac{1}{2^{N_{\text{site}}^{\text{hex}}} \prod_{\langle n, m \rangle} \cosh K_{nm}} Z_I^{\text{hex}}(P, P) = \frac{1}{\prod_n (1 + \Delta m_n)} \left[-Z_W^{\text{hex}}(P, P) + \sum_{\varepsilon \neq (P, P)} Z_W^{\text{hex}}(\varepsilon) \right], \quad (7)$$

$$\frac{1}{2 \prod_{\langle i, j \rangle} \exp L_{ij}} Z_I^{\text{tri}}(P, P) = \frac{1}{\prod_n (1 + \Delta m_n)} \left[+Z_W^{\text{hex}}(P, P) + \sum_{\varepsilon \neq (P, P)} Z_W^{\text{hex}}(\varepsilon) \right]. \quad (8)$$

Here, the couplings are identified as:

$$\frac{\kappa_{nm}}{\sqrt{(1 + \Delta m_n)(1 + \Delta m_m)}} \frac{\cos \Delta \alpha_{nmn'} \cos \Delta \alpha_{nmn''}}{\cos \Delta \alpha_{n'mn''}} = \tanh K_{nm} = e^{-2L_{ij}}, \quad (9)$$

where the angle differences $\Delta \alpha_{nmn'} \equiv \alpha_{nm} - \alpha_{mn'}$ are taken among the three neighboring sites from m : n , n' , and n'' . In eqs. (7) and (8), the boundary conditions are indicated by $\varepsilon = (P, P)$, (A, P) , (A, A) , (P, A) , where P stands for periodic and A for antiperiodic. Different signs for the (P, P) sector correspond to the sign ambiguity in defining the chirality operator in the Ising CFT [15, 8].

4. Staggered lattice structure in the affine-transformed hexagonal lattice

In Ref. [13], it was shown that the continuum limit can be taken under nontrivial affine transformation with the couplings:

$$\Delta m_n = 0, \quad \kappa_{n,n+\hat{k}} = \frac{2|\vec{\ell}_k|}{\sum_{k'} |\vec{\ell}_{k'}|}. \quad (10)$$

Although this is correct, it turns out that the bipartite hexagonal lattice shows a peculiar staggered structure under nontrivial affine transformation. While the directional information of the circum-center dual lattice, e_k , appears in the lattice action (2), the fermionic variables turn out to reside on a different lattice generically. This fine structure of the hexagonal lattice is relevant in deriving the lattice expression of the EM tensor as it involves a derivative in fermionic variables.

To see this, we consider the lattice equation of motion (EOM), $E_{\psi_n} = 0$, where

$$E_{\psi_n} = \psi_n - \frac{1}{2} \sum_k \kappa_k (1 - \vec{e}_k \cdot \vec{\sigma}) \psi_{n+\hat{k}} \quad (n : \text{even}), \quad (11)$$

$$E_{\psi_n} = \psi_n - \frac{1}{2} \sum_k \kappa_k (1 + \vec{e}_k \cdot \vec{\sigma}) \psi_{n-\hat{k}} \quad (n : \text{odd}). \quad (12)$$

The action is quadratic, and the infrared property of the Wilson-Dirac operator can be analyzed by the derivative expansion:

$$\psi_{n+\hat{k}} \simeq \psi_n + \ell'_{k\mu} \partial_\mu \psi_n, \quad (13)$$

where the translation vectors $\vec{\ell}'_k$ are arbitrary for now and to be determined below. For even sites:

$$\begin{aligned} E_{\psi_n} \simeq & \left(1 - \frac{1}{2} \sum_k \kappa_k\right) \psi_n + \frac{1}{2} \left(\sum_k \kappa_k e_{k\mu}\right) \sigma_\mu \psi_n \\ & - \frac{1}{2} \left(\sum_k \kappa_k \ell'_{k\mu}\right) \partial_\mu \psi_n + \frac{1}{2} \left(\sum_k \kappa_k e_{k\mu} \ell'_{k\nu}\right) \sigma_\mu \partial_\nu \psi_n, \end{aligned} \quad (14)$$

while for odd sites the signs of the second and third terms flip. The lattice EOM operators should approach the continuum expression:

$$E_\psi^{\text{cont}}(x) \equiv \sigma_\mu \partial_\mu \psi(x) \quad (15)$$

up to proportionality constant. Under the solution (10), this requirement reduces to the condition for the vectors $\vec{\ell}'_k$:

$$\sum_k \kappa_k \ell'_{k\mu} \equiv 0, \quad \sum_k \kappa_k e_{k\mu} \ell'_{k\nu} \equiv 2a \delta_{\mu\nu}, \quad (16)$$

where a scaling constant a can be set by demanding again the lattice dimension in the x direction to be unity. We have six conditions for six independent real variables (where an overall scaling is fixed by a), and the condition is sufficient to determine $\vec{\ell}'_k$.

As emphasized above, the solution $\vec{\ell}'_k$ to eq. (16) does not agree with $\vec{\ell}_k^*$ under a generic affine transformation. In Fig. 1, the two lattices are compared for the case $\tau = 1.2e^{4i\pi/9}$. We see that the lattice generated by $\vec{\ell}'_k$ has more regular appearance than that generated by $\vec{\ell}_k^*$.

5. Lattice operators

We are now ready to derive the lattice EM tensor in spin variables by applying parametric derivatives in the loop expansions. We first construct the lattice EM operators in the fermionic variables. Our basic building blocks are the following:

$$-\frac{\partial}{\partial \Delta m_n} \Big|_{\text{crit}} \langle \dots \rangle_{\text{conn}} = \left\langle \left(\frac{1}{2} \bar{\psi}_n \psi_n + 1 \right) \dots \right\rangle_{\text{conn}} \equiv \langle (\varepsilon_n + 1) \dots \rangle_{\text{conn}}, \quad (17)$$

$$\frac{\partial}{\partial \kappa_{nm}} \Big|_{\text{crit}} \langle \dots \rangle_{\text{conn}} = \left\langle \left(\bar{\psi}_n P(\vec{e}_{nm}) \psi_m \right) \dots \right\rangle_{\text{conn}} \equiv \langle E_{nm} \dots \rangle_{\text{conn}}, \quad (18)$$

where the dots represent other operator insertions in the path integral and $\langle \cdot \rangle_{\text{conn}}$ the connected part. The subscript ‘‘crit’’ emphasizes that we evaluate the derivatives at the critical couplings (10).

By a simple comparison between the lattice variable ψ_n and the continuum variable $\psi(x)$, the relative scaling can be determined. The ε operator can then be expressed as:

$$\varepsilon(x) \simeq \frac{2\pi}{a} \varepsilon_n \Leftrightarrow -\frac{2\pi}{a} \left[\frac{\partial}{\partial \Delta m_n} \Big|_{\text{crit}} - 1 \right]. \quad (19)$$

As for the EM tensor, we consider the projected tensor:

$$T_k(x) \equiv -\frac{1}{2} e'_{k\mu} e_{k\nu} \bar{\psi}(x) \sigma_\mu \partial_\nu \psi(x), \quad (20)$$

for which we have the lattice expression:

$$\begin{aligned} T_k(x) &\simeq \frac{2\pi}{a} \frac{1}{|\vec{\ell}'_k|} \left[E_{n,n+\hat{k}} - \frac{1}{2} (\varepsilon_n + \varepsilon_{n+\hat{k}}) \right] \\ &\Leftrightarrow \frac{2\pi}{a} \frac{1}{|\vec{\ell}'_k|} \left[\frac{\partial}{\partial \kappa_{n,n+\hat{k}}} + \frac{1}{2} \left(\frac{\partial}{\partial \Delta m_n} + \frac{\partial}{\partial \Delta m_{n+\hat{k}}} \right) - 1 \right] \Big|_{\text{crit}}. \end{aligned} \quad (21)$$

The unit vectors $\vec{e}'_k \equiv \vec{\ell}'_k / |\ell'_k| \equiv (\cos \alpha'_k, \sin \alpha'_k)^T$ encode the angle information of the $\vec{\ell}'_k$ -lattice. Up to the EOM, $T_k(x)$ can be expressed as a linear combination of the holomorphic part $T(z)$ and the antiholomorphic part $\tilde{T}(\bar{z})$:

$$T_k(x) = \frac{1}{2} \left[\cos(\alpha'_k + \alpha_k^*) T(z) - \sin(\alpha'_k + \alpha_k^*) \tilde{T}(\bar{z}) \right]. \quad (22)$$

Thus, the set $T_k(x)$ ($k = 1, 2, 3$) is sufficient to reconstruct all the components of the EM tensor.

Having obtained the lattice operators expressed with the parametric derivatives, they can be readily mapped to the spin systems via loop expansions (7) and (8). On the hexagonal lattice, the building blocks (17) and (18) correspond to:

$$\varepsilon_n = \sum_k \tanh K_{n,n+\hat{k}} \cosh^2 K_{n,n+\hat{k}} \left(\frac{1}{2} \mu_n \mu_m + \tanh K_{n,n+\hat{k}} \right) + 1, \quad (23)$$

$$E_{n,n+\hat{k}} = \frac{\tanh K_{n,n+\hat{k}} \cosh^2 K_{n,n+\hat{k}}}{\kappa_{n,n+\hat{k}}} \mu_n \mu_{n+\hat{k}}, \quad (24)$$

while on the triangular lattice:

$$\varepsilon_n = \sum_{\langle i,j \rangle \text{ around } n} s_i s_j - 2, \quad (25)$$

$$E_{n,n+\hat{k}} = -\frac{1}{2} \frac{1}{\kappa_{n,n+\hat{k}}} s_i s_j. \quad (26)$$

In eq. (25), the sum is over the links $\langle i, j \rangle$ on the triangular lattice surrounding the hexagonal site n , while in eq. (26), the link $\langle i, j \rangle$ on the triangular lattice intersects with the link $\langle n, n + \hat{k} \rangle$ on the hexagonal lattice. The lattice operators for the CFT, $\varepsilon(x)$ and $T_k(x)$, can then be constructed by the same linear combinations (19) and (21).

We comment that both $\varepsilon(x)$ and $T_k(x)$ acquire divergent parts through loop diagrams (the divergent part of $\varepsilon(x)$ comes from the Wilson term). The divergent parts need to be subtracted when we consider disconnected components. This corresponds to taking the normal ordering. For the Ising CFT, its evaluation can be performed with the fermion system without statistical error [8]. In the numerical analysis below, all the lattice operators are regularized in this way.

6. Confirming the CFT formulas with Monte Carlo calculations

In this section, we calculate various expectation values that involve the EM tensor with the spin variable by performing Monte Carlo calculation. Ensembles are generated by combining the Wolff algorithm [12] with the local heat-bath algorithm. The details of the calculation will be described in Ref. [8]. We comment that the signal of the EM tensor is noisy as the contributions from 1 (the diverging part), $\varepsilon(x)$, and $\partial\varepsilon(x)$ (the first descendant of $\varepsilon(x)$) need to be subtracted to single out the EM tensor components. The exact values are evaluated with the analytic expressions known in the Ising CFT [5, 6]. The modulus is set to a nontrivial value $\tau = 1.2e^{4i\pi/9}$ below.

We begin with the one-point function of the EM tensor. In Fig. 2, we show the results of $\langle T_k(x) \rangle$ on the hexagonal lattice. For completeness, a constant fit is performed for the three points, $L = 10, 12, 14$, to make a comparison with the exact value. The obtained values are:

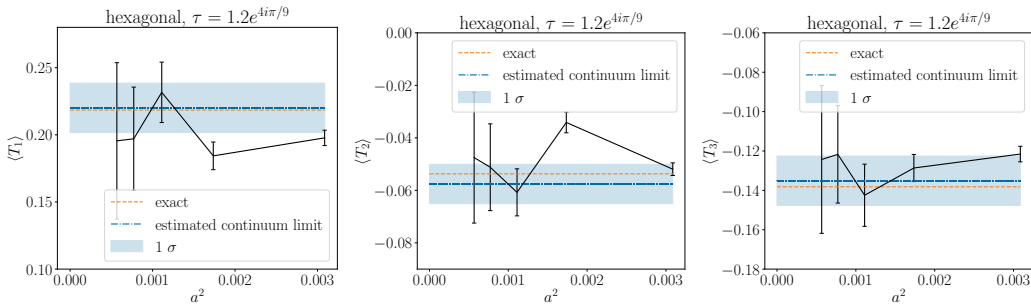


Figure 2: Extrapolation of $\langle T_k \rangle$ ($k = 1, 2, 3$) to the continuum limit for $\tau = 1.2e^{4i\pi/9}$ on the hexagonal lattice for $L = 6, 8, \dots, 14$.

$\langle T_1 \rangle \approx 0.215(21)$ (exact: 0.218), $\langle T_2 \rangle \approx -0.0605(88)$ (exact: -0.0537), $\langle T_3 \rangle \approx -0.126(15)$ (exact: -0.138). The good agreement shows that we have a good understanding of the lattice operators including the mixing angle between T and \tilde{T} [see eq. (22)], the diverging part, and the normalization.

We next consider the three-point function with the spin operators. This is the least noisy correlator involving the EM tensor. Recall that the conformal Ward identity for the primary fields $\phi_i(z, \bar{z})$ with the conformal weights (h_i, \tilde{h}_i) is [5]:

$$\begin{aligned} & \langle T(z)\phi_1(z_1, \bar{z}_1) \cdots \phi_N(z_N, \bar{z}_N) \rangle - \langle T(z) \rangle \langle \phi_1(z_1, \bar{z}_1) \cdots \phi_N(z_N, \bar{z}_N) \rangle \\ &= \left\{ 2\pi i \partial_\tau + \sum_{i=0}^N \left[h_i \{ \wp(z_i - z) + 2\eta_1 \} + \{ -\zeta(z_i - z) + 2\eta_1(z_i - z) + \pi i \} \partial_{z_i} \right] \right\} \times \\ & \quad \times \langle \phi_1(z_1, \bar{z}_1) \cdots \phi_N(z_N, \bar{z}_N) \rangle, \end{aligned} \quad (27)$$

where $\wp(z)$ and $\zeta(z)$ are the Weierstrass functions and $\eta_1 \equiv \zeta(\omega_1)$ ($\omega_1 \equiv \tau/2$). We see that as $T_k(x)$ approaches the location of the other primary operators, it exhibits a diverging pole structure of order two, giving rise to a complex global landscape in its functional form. For this reason, to compare the lattice correlators with the exact values, we look into their sign pattern on the entire torus. Figure 3 shows the result for $\langle T_k(x)\mu(0)\mu(\omega_3) \rangle$ ($\omega_3 \equiv (1 + \tau)/2$) on the hexagonal lattice with $L = 14$. Though we observe a cutoff effect away from the insertion points x_i , we observe an

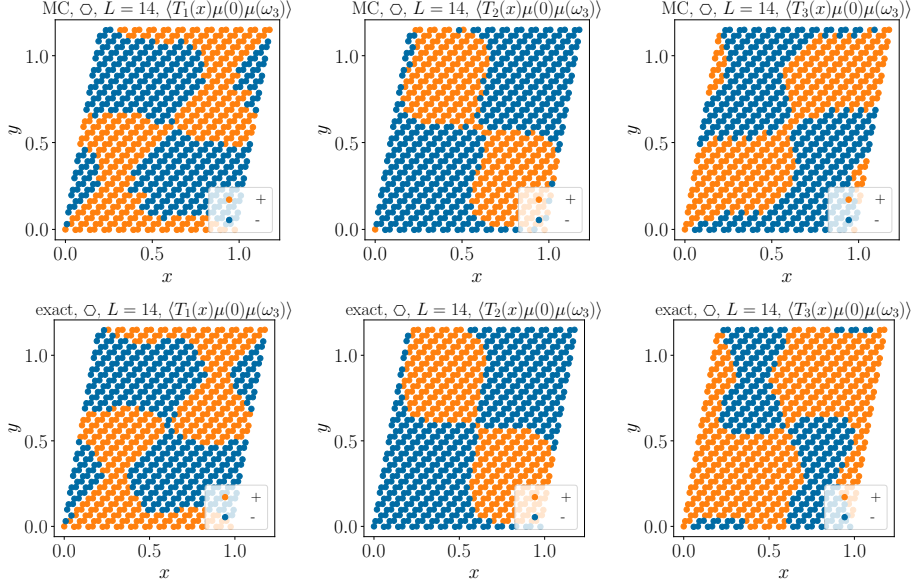


Figure 3: The sign patterns of $\langle T_k(x)\mu(0)\mu(\omega_3) \rangle$ on the hexagonal lattice. Monte Carlo result (top) and the exact solution (bottom) with $\tau = 1.2e^{4i\pi/9}$, $L = 14$, and $\omega_3 = (1 + \tau)/2$. $k = 1, 2, 3$ from left to right.

agreement in the global landscape, in particular the characteristic pole structure.

Finally, we calculate the TT -correlator, which cannot be re-expressed with the primary correlators by the conformal Ward identity. In Fig. 4, we show the $\langle T_k(x)T_2(0) \rangle$ correlators on the triangular lattice for $L = 10$. We comment that the signal turns out to be less noisy on the triangular lattice than on the hexagonal lattice for a given L (note, however, that the number of lattice sites is half on the triangular lattice). We again confirm the correct landscape of the correlator with statistical noise at the edge of \pm patterns.

From the above results, we see that the derived lattice EM tensor correctly sources the desired CFT operator both on hexagonal and triangular lattices under generic affine transformation.

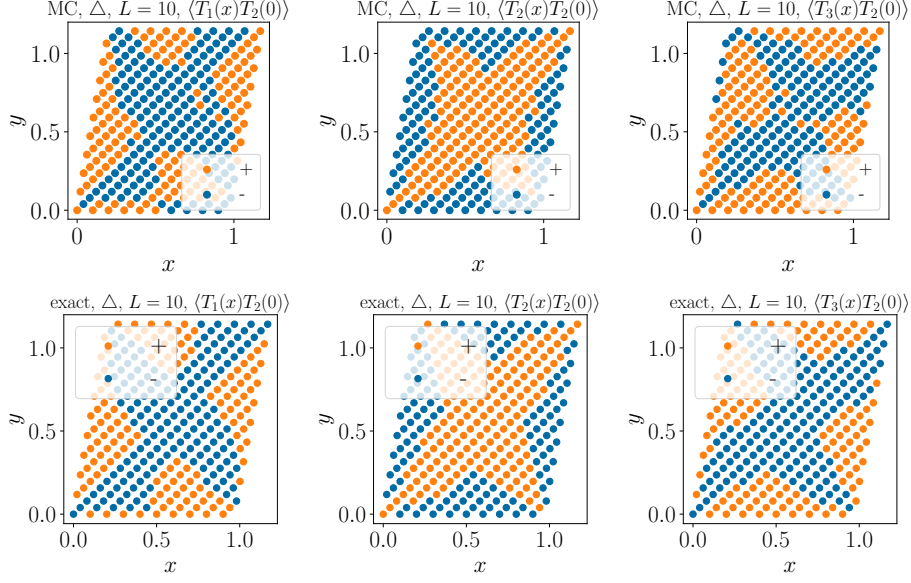


Figure 4: The sign patterns of $\langle T_k(x)T_2(0) \rangle$ ($k = 1, 2, 3$) plotted for the Monte Carlo result (top) and the exact solution (bottom) with $\tau = 1.2e^{4i\pi/9}$, $L = 6$ on the hexagonal lattice.

7. Conclusion

In this contribution, we derived the lattice EM tensor for the Ising CFT with spin variables on triangular and hexagonal lattices under generic affine transformation. We numerically confirmed that the expression correctly sources the CFT operator. It shows our understanding is correct on the mixing angle between T and \tilde{T} in relation to the staggered lattice structure, the identification of the divergent part, and the operator normalization. Evaluation of the one-point function is of particular importance in curved space applications as it measures the trace anomaly proportional to the curvature. We believe that this work gives an important step towards studying the CFT on curved lattices.

Acknowledgments

The authors thank Hidenori Fukaya, Okuto Morikawa, and Yusuke Namekawa for valuable discussions in LATTICE 2024. This work is partially supported by the Scientific Discovery through Advanced Computing (SciDAC) program, “Multiscale acceleration: Powering future discoveries in High Energy Physics” under FOA LAB-2580 funded by the U.S. DOE, Office of Science, and DOE under Award DE-SC0015845. The computation was performed on the Shared Computing Cluster (SCC) which is administered by Boston University’s Research Computing Services [16].

References

- [1] R. C. Brower, G. Fleming, A. Gasbarro, T. Raben, C.-I. Tan, and E. Weinberg, *Quantum Finite Elements for Lattice Field Theory*, PoS **LATTICE2015**, 296 (2016), arXiv:1601.01367 [hep-lat].
- [2] S. Fubini, A. J. Hanson, and R. Jackiw, *New approach to field theory*, Phys. Rev. D **7**, 1732 (1973).
- [3] J. L. Cardy, *Universal amplitudes in finite-size scaling: generalisation to arbitrary dimensionality*, J. Phys. A **18**, L757 (1985).
- [4] R. C. Brower, G. T. Fleming, and H. Neuberger, *Lattice Radial Quantization: 3D Ising*, Phys. Lett. B **721**, 299 (2013), arXiv:1212.6190 [hep-lat].
- [5] T. Eguchi and H. Ooguri, *Conformal and Current Algebras on General Riemann Surface*, Nucl. Phys. B **282**, 308 (1987).
- [6] P. Di Francesco, H. Saleur, and J. B. Zuber, *Critical Ising Correlation Functions in the Plane and on the Torus*, Nucl. Phys. B **290**, 527 (1987).
- [7] L. P. Kadanoff and H. Ceva, *Determination of an operator algebra for the two-dimensional Ising model*, Phys. Rev. B **3**, 3918 (1971).
- [8] R. C. Brower, G. T. Fleming, N. Matsumoto, and R. Misra, *in preparation*.
- [9] L. Onsager, *Crystal statistics. i. a two-dimensional model with an order-disorder transition*, Phys. Rev. **65**, 117 (1944).
- [10] T. D. SCHULTZ, D. C. MATTIS, and E. H. LIEB, *Two-dimensional ising model as a soluble problem of many fermions*, Rev. Mod. Phys. **36**, 856 (1964).
- [11] C. Itzykson, *ISING FERMIONS. 1. TWO-DIMENSIONS*, Nucl. Phys. B **210**, 448 (1982).
- [12] U. Wolff, *Ising model as Wilson-Majorana Fermions*, Nucl. Phys. B **955**, 115061 (2020), arXiv:2003.01579 [hep-lat].
- [13] R. C. Brower and E. K. Owen, *Ising model on the affine plane*, Phys. Rev. D **108**, 014511 (2023), arXiv:2209.15546 [hep-th].
- [14] S. Samuel, *The use of anticommuting variable integrals in statistical mechanics. i. the computation of partition functions*, Journal of Mathematical Physics **21**, 2806 (1980).
- [15] N. Seiberg and E. Witten, *Spin Structures in String Theory*, Nucl. Phys. B **276**, 272 (1986).
- [16] *Shared Computing Cluster (SCC)*, www.bu.edu/tech/support/research/.